

On Sequential Maximum a Posteriori Inference for Continual Learning

Menghao Waiyan William Zhu[✉]
Tsinghua Shenzhen International Graduate School
Shenzhen, China
zhumh22@mails.tsinghua.edu.cn

Ercan Engin Kuruoğlu
Tsinghua Shenzhen International Graduate School
Shenzhen, China
kuruoglu@sz.tsinghua.edu.cn

Abstract—We formulate sequential maximum a posteriori inference as a recursion of loss functions and reduce the problem of continual learning to approximating the previous loss function. We then propose two coreset-free methods: autodiff quadratic consolidation, which uses an accurate and full quadratic approximation, and neural consolidation, which uses a neural network approximation. These methods are not scalable with respect to the neural network size, and we study them for classification tasks in combination with a fixed pre-trained feature extractor. We also introduce simple but challenging classical task sequences based on Iris and Wine datasets. We find that neural consolidation performs well in the classical task sequences, where the input dimension is small, while autodiff quadratic consolidation performs consistently well in image task sequences with a fixed pre-trained feature extractor, achieving comparable performance to joint maximum a posteriori training in many cases.

Index Terms—Bayesian inference, class-incremental learning, continual learning, domain-incremental learning, neural networks

I. INTRODUCTION

When a neural network (including a generalized linear model, which is essentially a neural network with no hidden layers) is trained on a task and fine-tuned on a new task, it loses predictive performance on the old task. This is known as catastrophic forgetting [1] and can be prevented by training jointly on all tasks, but the previous data may not be accessible due to computational or privacy constraints. Thus, we would like to learn from a sequence of tasks with limited or no access to the previous data. This is known as continual learning or incremental learning or lifelong learning.

For classification tasks, three types of continual learning settings are commonly studied [2]:

- 1) Task-incremental learning, in which task IDs are provided and the classes change between tasks
- 2) Domain-incremental learning, in which task IDs are not provided and the classes remain the same between tasks but the input data distribution changes between tasks
- 3) Class-incremental learning, in which task IDs are not provided and the classes change between tasks

For example, Split MNIST is a sequence of five tasks created from the MNIST dataset, in which the first task consists of images of zeros and ones, the second task consists of images of twos and threes and so on. In the task-incremental setting, the task IDs 1-5 are provided, and the neural network only

has to decide between two classes for each task ID. Typically, a multi-headed neural network with five heads (one head for each task) is used in this setting. In the domain-incremental setting, the task is classification of even and odd digits without access to the task ID. In the class-incremental setting, the task is classification of all ten digits without access to the task ID. In these settings, a single-headed neural network is typically used.

Task-incremental learning has been criticized as task IDs make the problem of continual learning easier [3]. In fact, if there is only one class per task, then the task ID could be used to make a perfect prediction. Moreover, in practice, it is unlikely that task IDs are accessible. For example, in Split MNIST, we would like to classify all ten digits in the end rather than just tell which of the two digits in each task. In accordance with the desiderata proposed in [3], we focus on domain- and class-incremental learning with single-headed neural networks on task sequences with more than two similar tasks and no access to the previous data.

For a single-headed neural network with fixed architecture, the learning problem can be formulated as Bayesian inference on the neural network parameters. Then, sequential Bayesian inference provides an elegant approach to continual learning. In particular, continual learning can be done by using the previous posterior distribution as the current prior distribution. If full Bayesian prediction is used, then the approach is known as a Bayesian neural network. In our work, we focus on maximum a posteriori (MAP) prediction, which uses only the maximum point of the posterior distribution. By defining the loss function as the negative log joint probability density function (PDF), this leads to a recursive formulation of loss functions, and the problem is reduced to approximating the previous loss function.

When adult humans learn to recognize new objects, they have already learned similar objects before, and they do not need to continually learn low-level features such as edges, corners and shapes. This suggests that the low-level layers of a neural network should be fixed after learning on a similar task, and then the neural network can be used as a feature extractor. For example, a neural network pre-trained on handwritten letters can be used as a feature extractor for continual learning on handwritten digits.

Our goals are to investigate the continual learning perfor-

mance of a full quadratic approximation and a neural network approximation of the previous loss functions and the effect of using a pre-trained feature extractor for sequential MAP inference.

II. SEQUENTIAL MAXIMUM A POSTERIORI INFERENCE

We describe our probabilistic model for continual learning and how sequential MAP inference based on it leads to a recursion of loss functions. Then, we propose two methods for approximating the previous loss function: autodiff quadratic consolidation (AQC), which uses an accurate and full quadratic approximation, and neural consolidation (NC), which uses a neural network approximation. Finally, we discuss their limitations.

A. Probabilistic Model

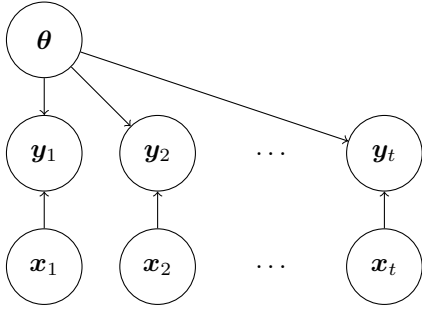


Fig. 1: Bayesian network for continual learning. θ is the collection of parameters of the neural network, $x_{1:t}$ are the inputs and $y_{1:t}$ are the outputs.

Let θ be the collection of parameters of the neural network and $x_{1:t}$ and $y_{1:t}$ be the inputs and outputs from time 1 to t , respectively. $x_{1:t}$ are assumed to be independent, and $y_{1:t}$ are assumed to be conditionally independent given θ and $x_{1:t}$. These assumptions are depicted in Fig. 1.

$(x, y)_{1:t}$ are not necessarily identically distributed. However, it is assumed that tasks are similar, i.e. the form of the likelihood function $l_t(y_t|\theta, x_t)$ is the same for all tasks. For example, in multi-class classification, it is the categorical likelihood function for all tasks.

After observing $(x, y)_{1:t} = (x, y)_{1:t}$ at time t , the posterior PDF is

$$p_t(\theta|x_{1:t}, y_{1:t}) = \frac{1}{z_t} p_{t-1}(\theta|x_{1:t-1}, y_{1:t-1}) l_t(y_t|\theta, x_t) \quad (1)$$

where $z_t = \int_{\Theta} p_{t-1}(\theta|x_{1:t-1}, y_{1:t-1}) l_t(y_t|\theta, x_t) d\theta$ is a normalization term which does not depend on θ . MAP prediction uses the maximum of the posterior PDF to make a prediction $f(x; \theta_t^*)$, where f is the neural network function, x is the input and θ_t^* is the MAP estimate at time t .

Since multiplying by a constant does not affect the minimum, the loss function \mathcal{L}_t at time t can be defined as the negative log joint PDF $-\ln j_t(\theta, y_{1:t}|x_{1:t})$ at time t . Then, the minimum of the loss function is equivalent to the

MAP estimate, and we have a recursion of loss functions for $t = 1, 2, \dots$:

$$\mathcal{L}_t(\theta) = \mathcal{L}_{t-1}(\theta) + l_t(\theta) \quad (2)$$

where l_t is the negative log likelihood (NLL) at time t . For binary classification, where the likelihood is assumed to be Bernoulli, l_t is the binary or Bernoulli cross entropy, while for multi-class classification, where the likelihood is assumed to be categorical, l_t is the categorical cross entropy. \mathcal{L}_0 is the negative log (un-normalized) prior at time 1, e.g., $\frac{1}{2}\|\theta\|^2$ for the standard Gaussian prior.

In Eq. (2), \mathcal{L}_{t-1} depends on the previous data $(x, y)_{1:t-1}$ and l_t depends on the current data $(x, y)_t$. Forgetting happens when we minimize only l_t but ignore \mathcal{L}_{t-1} as in fine-tuning. In joint MAP training, all the data are used, so \mathcal{L}_t is effectively minimized. If there is no access to the previous data, then \mathcal{L}_{t-1} must be approximated. We investigate two ways to approximate it, namely quadratic approximation and neural network approximation.

B. Autodiff Quadratic Consolidation

A quadratic approximation of \mathcal{L}_{t-1} corresponds to a Laplace approximation of the posterior PDF at time $t-1$. The quadratic approximation is a second-order Taylor series approximation around θ_{t-1}^* , where the gradient is zero, so the linear term disappears. Moreover, the constant term does not affect the PDF. Thus, the approximation consists of a single quadratic term of the form $\frac{1}{2}(\theta - \theta_{t-1}^*)^T H(l_{t-1})(\theta_{t-1}^*)(\theta - \theta_{t-1}^*)$, where $H(l_{t-1})(\theta_{t-1}^*)$ is the Hessian matrix of the NLL of task $t-1$ at θ_{t-1}^* . [4] shows that successive quadratic approximation results in addition of the Hessian matrices of the NLL of the previous tasks at the corresponding minima. Thus, the approximate loss function is

$$\hat{\mathcal{L}}_t(\theta) = \frac{\lambda}{2}(\theta - \theta_{t-1}^*)^T \left(\sum_{i=0}^{t-1} H(l_i)(\theta_i^*) \right) (\theta - \theta_{t-1}^*) + l_t(\theta) \quad (3)$$

where λ is a positive real number introduced as a hyperparameter.

The Hessian matrix is the transpose of the Jacobian matrix of the gradient: $H(f)(x) = (J(\nabla f)(x))^T$ for any twice differentiable point x of a function f . In most cases, the NLL l_{t-1} is twice continuously differentiable, so the Hessian matrix at its minimum is symmetric positive definite. Then, it can be implemented as $J(\nabla l_{t-1})(\theta_{t-1}^*)$, the Jacobian matrix of its gradient at its minimum, by using automatic differentiation.

Since the Hessian operator is linear, the Hessian matrix of the batch negative log likelihood is equal to the sum of the Hessian matrices of the mini-batch negative log likelihood:

$$H(l_{t-1})(\theta_{t-1}^*) = H \left(\sum_{j=1}^b l_{t-1,j} \right) (\theta_{t-1}^*) = \sum_{j=1}^b H(l_{t-1,j})(\theta_{t-1}^*) \quad (4)$$

where $l_{t-1,j}$ is the mini-batch negative log likelihood of the j -th mini-batch at time $t-1$.

The above trick allows working with a large dataset by dividing it into small mini-batches. However, if the neural network is large, i.e. θ has a large amount of parameters, then the computation may become intractable.

The training for each task thus consists of three steps:

- 1) If it is the first task, then the loss function is set to $\frac{1}{2}\|\theta\|^2 + l_1(\theta)$ assuming a standard Gaussian prior; otherwise, it is updated as in Eq. (3) with the MAP estimate θ_{t-1}^* and the Hessian matrix $H_{t-1} = \sum_{i=0}^{t-1} H(l_i)(\theta_i^*)$ of the previous task.
- 2) Training is done on the loss function using mini-batch gradient descent, and the regularization term is scaled by dividing by the number of mini-batches in the dataset.
- 3) The Hessian matrix for the current task is computed and added to that of the previous task $H_t = H_{t-1} + H(l_t)(\theta_t^*)$, and the current MAP estimate θ_t^* and Hessian matrix H_t are stored in order to be used to update the next loss function.

This method is referred to as Autodiff Quadratic Consolidation (AQC).

C. Neural Consolidation

A neural network approximation uses a consolidator neural network κ with parameters ϕ_{t-1}^* . The approximate loss function is

$$\hat{\mathcal{L}}_t(\theta) = \lambda \kappa(\theta; \phi_{t-1}^*) + l_t(\theta) \quad (5)$$

where λ is a positive real number introduced as a hyperparameter and ϕ_{t-1}^* is the collection of trained parameters of the consolidator neural network at time $t-1$.

The consolidator neural network is trained by minimizing an L^2 -regularized Huber loss function to fit it to the previous loss function with a sample generated uniformly within a ball of radius r around θ_{t-1}^* at each gradient descent step. If n points are generated, then the consolidator loss function is

$$\mathcal{L}_{t-1,\kappa}(\phi) = \frac{1}{2}\beta\|\phi\|_2^2 + \sum_{i=1}^n h_{t-1,i}(\phi) \quad (6)$$

where β is a positive real number introduced as a hyperparameter and $h_{t-1,i}(\phi)$ is the Huber loss function with respect to $\hat{\mathcal{L}}_{t-1}(\theta_i)$ and $\kappa(\theta_i; \phi)$. If the dataset is very large, $\hat{\mathcal{L}}_{t-1}$ can be computed on the sample in mini-batches and added.

The training for each task thus consists of three steps:

- 1) If it is the first task, then the loss function is set to $\frac{1}{2}\|\theta\|^2 + l_1(\theta)$ assuming a standard Gaussian prior; otherwise, it is updated as in Eq. (5) with the parameters ϕ_{t-1}^* of the consolidator neural network of the previous task.
- 2) Training is done on the loss function using mini-batch gradient descent, and the regularization term is scaled by dividing by the number of mini-batches in the dataset.
- 3) The consolidator neural network is trained by performing gradient descent on Eq. (6) with a sample of n points of θ generated uniformly within a ball of radius r around θ_t^* at each step as described above, and the parameters

ϕ_t^* of the consolidator neural network are stored in order to be used to update the next loss function.

This method is referred to as Neural Consolidation (NC).

D. Limitations

As in all single-headed approaches, the total number of classes must be known in advance. The main limitation of AQC and NC is that they are not scalable with respect to the neural network size although they can be used when the datasets are large. This limitation may be overcome by using a fixed feature extractor pre-trained on a similar task and performing continual learning with one dense layer on the features. Finally, both continual learning methods are sensitive to hyperparameters, so a validation dataset sequence should be used to perform hyperparameter tuning.

III. RELATED WORK

There are several continual learning methods which are based on sequential MAP inference and use quadratic approximation of the previous loss function. Elastic weight consolidation (EWC) approximates the Hessian matrix by using a diagonal approximation of the empirical Fisher information matrix (eFIM) [5]. The original EWC adds a quadratic term to the objective for every task. [6] proposes a corrected objective with a single quadratic term for which the eFIM can be cumulatively added. There is another variant called EWC++ [7], which performs a convex combination of the previous and current eFIMs instead of adding them. Synaptic intelligence (SI) performs a diagonal approximation of the Hessian matrix by using the change in loss during gradient descent [8]. Online structured Laplace approximation uses Kronecker factorization to perform a block-diagonal approximation of the Hessian matrix, in which the diagonal blocks of the matrix correspond to a layer of the neural network [9].

Another class of methods that are not based on sequential MAP inference but are based on sequential Bayesian inference is sequential variational inference. It approximates the posterior distribution with a variational distribution, which is a simple parametric distribution, typically a Gaussian or a Gaussian mixture distribution, by minimizing an objective called the variational free energy or the negative evidence lower bound with respect to the parameters of the variational distribution. It uses the whole posterior distribution rather than a point from it to make predictions. Gaussian variational continual learning (G-VCL) [10] and Gaussian mixture variational continual learning (GM-VCL) [11] approximate the posterior distribution over the parameters with a Gaussian distribution and a Gaussian mixture distribution, respectively. Gaussian sequential function space variational inference (G-SFSVI) [12] approximates the posterior distribution over the outputs (before the final activation function) of a selected number of inputs called inducing points with a Gaussian distribution.

Pre-training for initialization and pre-training for feature extraction have both been empirically shown to improve continual learning. In the former, the pre-trained parameters are used as the initial parameters for continual learning [13],

[14]. In the latter, the pre-trained neural network is used as a feature extractor [15]–[17].

We investigate the continual learning performance of AQC, which is the most accurate form of quadratic approximation of the previous loss function, and NC, which is a neural network approximation of the previous loss function. In image classification tasks, we use a fixed feature extractor pre-trained on a similar task and perform continual learning with one dense layer on the features.

IV. EXPERIMENTS

Experiments are performed on classical task sequences as well as image task sequences. In each experiment, the final average accuracy of AQC and NC are compared with reference methods, sequential variational inference methods and sequential MAP inference methods. Each task sequence has a training dataset sequence, validation dataset sequence and testing dataset sequence. The validation dataset sequence is used to perform hyperparameter tuning via grid search. Descriptions of data used and methods compared as well as a discussion of results are provided below, and more details are provided in Appendix A.

A. Data

The task sequences for continual learning as well as the tasks for pre-training are listed below. The classical task sequences that we introduce here might seem simple, but they are challenging task sequences for continual learning. In all task sequences, CI indicates that it is for class-incremental learning, while DI indicates that it is for domain-incremental learning.

- Classical Task Sequences

- **CI Split Iris:** Iris is a task for classification of 3 species of flowers based on 4 features. It is split into 3 tasks for learning 1 species at a time. CI Split 2D Iris is a task sequence for visualization derived from it by selecting two features "petal length" and "petal width".
- **CI Split Wine:** Wine is a task for classification of 3 classes of wine based on 13 features. It is split into 3 tasks for learning 1 class at a time.

- Image task sequences

- **CI Split MNIST:** MNIST is a task for classification of 10 classes of digits based on grayscale images of handwritten digits. It is split into 5 tasks for learning 2 classes at a time.
- **CI Split CIFAR-10:** CIFAR-10 is a task for classification of 10 classes of natural objects based on images. It is split into 5 tasks for learning 2 classes at a time.
- **CI Split HAM-8:** HAM10000 is a task for classification of 8 classes of skin conditions based on dermatoscopic images. It is renamed to HAM-8 based on the number of classes and split into 4 tasks for learning 2 classes at a time.

- **DI Split MNIST:** MNIST is split into 5 tasks with 2 classes at a time, but each task is of binary classification of even and odd digits.
- **DI Split CIFAR-8:** CIFAR-10 has 6 types of animal and 4 types of vehicle, so 2 types of animal ("bird" and "frog") are removed to make CIFAR-8, which is then split into 4 tasks with 2 classes at a time, but each task is of binary classification of vehicles and animals.
- **DI Split HAM-6:** HAM-8 has 4 types of benign skin condition, 1 type of indeterminate skin condition and 3 types of malignant skin condition, so 1 type of benign skin condition ("vascular lesion") and 1 type of indeterminate skin condition ("actinic keratosis") are removed to make HAM-6, which is then split into 3 tasks with 2 classes at a time, but each task is of binary classification of benign and malignant skin conditions.

- Pre-training Tasks

- **EMNIST Letters:** EMNIST Letters is a task for classification of 26 classes of letters based on grayscale images of handwritten letters. It has no classes in common with MNIST and is used for pre-training for CI Split MNIST and DI Split MNIST.
- **CIFAR-100:** CIFAR-100 is a task for classification of 100 classes of natural objects based on images. It has no classes in common with CIFAR-10 and is used for pre-training for CI Split CIFAR-10 and DI Split CIFAR-10.
- **BCN-12:** BCN20000 is a task for classification of 8 classes of skin conditions based on dermatoscopic images. It is renamed to BCN-12 based on the number of classes. Most classes are in common with HAM-8, but the images are from different populations. It is used for pre-training for CI Split MNIST and DI Split MNIST.

B. Methods

We compare AQC and NC with reference methods, sequential variational inference methods and sequential MAP inference methods. Joint MAP training and fine-tuning serve as the best and worst reference methods, respectively. In the former, all the previous data are used together with the current data to train the neural network, while in the latter, the previously trained neural network is simply fine-tuned to the current task. The variational inference methods compared are G-VCL [10], GM-VCL [11] and G-SFSVI [12], and the sequential MAP inference methods compared are EWC with Huszár's corrected penalty [4], [6] and SI [8]. These methods are described in Section III. To make fair comparisons, only coreset-free methods, i.e. methods do not store any previous data, are considered.

Each method runs through each training dataset sequence, its hyperparameters are selected based on the final average accuracy on the validation dataset sequence, and it is evaluated based on the final average accuracy on the testing dataset

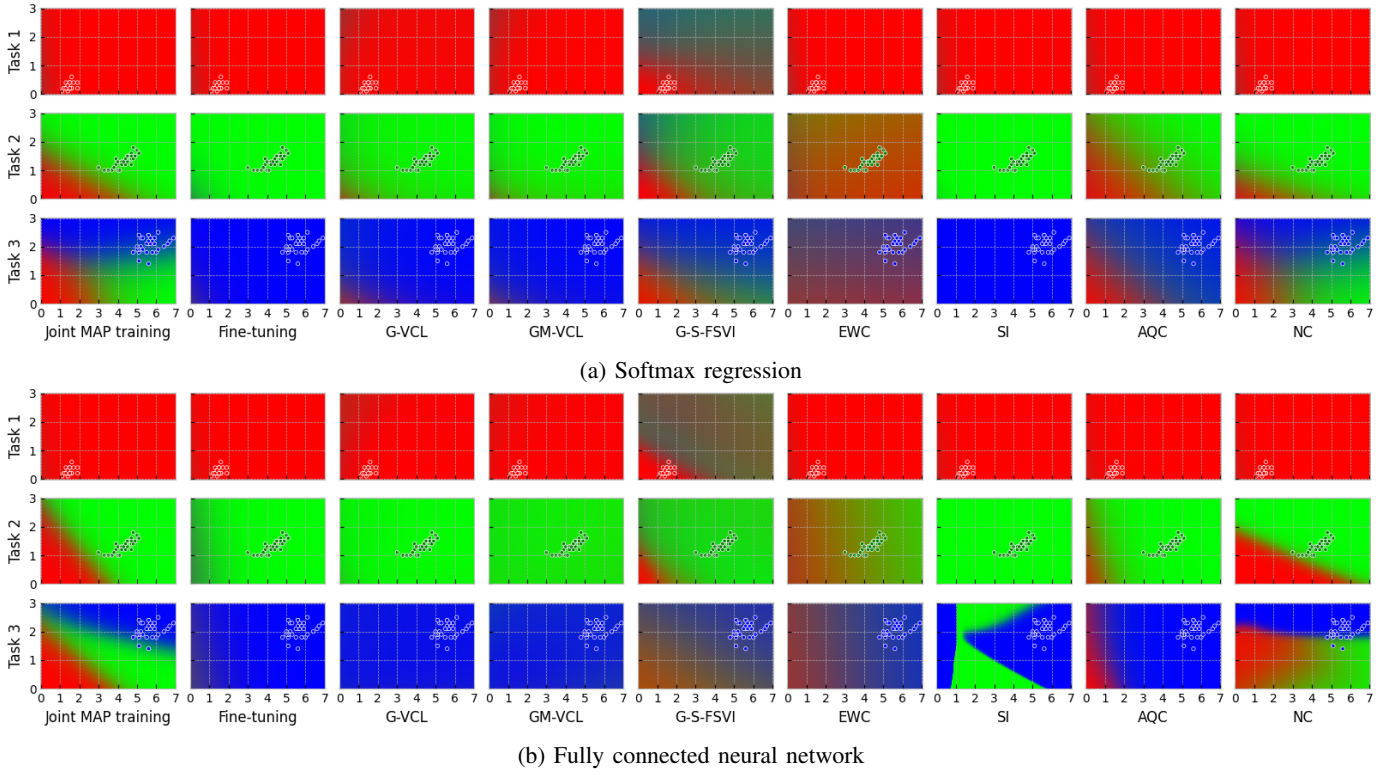


Fig. 2: Visualizations of prediction probabilities for the methods on CI Split 2D Iris. The x-axis is the petal length (cm) and the y-axis is the petal width (cm). The pseudocolor plot shows the prediction probabilities, where the 3 class probabilities are mapped to the red, green and blue values, respectively, and the dots show the observed data. NC performs the best and is better with softmax regression.

sequence. The final average accuracy on a dataset sequence is defined as the average of all the accuracies on all the datasets in the sequence.

C. Results

Since AQC relies on the very accurate automatic differentiation for Hessian computation, we expect that it has better final average accuracy than EWC and SI, and we are interested in observing how much better it performs. Since neural networks are powerful function approximators, and the previous loss functions in our experiments are not quadratic, we expect that NC has better final average than the quadratic approximation methods. We are also interested in how much a pre-trained feature extractor helps in sequential MAP inference.

Visualizations of the prediction probabilities for the methods on CI Split 2D Iris for softmax regression and a fully connected neural network are shown in Fig. 2. We find that AQC performs better than EWC and SI, and NC performs the best, but it does better for softmax regression.

The testing final average accuracies for the methods on classical and image task sequences are shown in Table I. We find that AQC performs better than EWC and SI, and NC performs the best in most classical task sequences. We also find that NC performs better with softmax regression than with a fully connected neural network probably because

the loss function in the former is convex and is easier to fit. In image task sequences, where a feature extractor is used, AQC consistently performs the best and has performance comparable to joint MAP training in some task sequences. However, we find that NC does not perform as well as AQC, but is better than EWC and SI in some task sequences.

It is notable that EWC performs as poorly as fine-tuning in class-incremental learning on the whole neural network from scratch [2], but using a pre-trained feature extractor significantly improves it. Moreover, in DI Split CIFAR-8, using a pre-trained feature extractor alone significantly reduces forgetting, and even fine-tuning performs quite well.

A possible reason that NC does not perform well in image task sequences is that the dimension of the feature space is high (64 in CI Split MNIST and DI Split MNIST and 512 in other task sequences), and random sampling becomes inefficient in high dimensions.

D. Data Availability

All the datasets used in this work are publicly available. Iris and Wine are available from the `scikit-learn` package [18], which is released under the 3-clause BSD license. MNIST, EMNIST, CIFAR-10 and CIFAR-100 are available from the `pytorch` package [19], which is also released under the 3-clause BSD license. HAM10000 [20] is released

TABLE I: Testing final average accuracy for the methods on classical and image task sequences. For classical task sequences, results for softmax regression (SR) and a fully connected neural network (FCNN) are shown. Pre-training on a similar task is used for image task sequences. NC performs the best in most classical task sequences while AQC performs the best in all image task sequences with a fixed pre-trained feature extractor.

(a) Classical task sequences

Method	CI Split Iris SR	CI Split Iris FCNN	CI Split Wine SR	CI Split Wine FCNN
Joint MAP training	96.6667	100.0000	91.1111	91.1111
Fine-tuning	33.3333	33.3333	33.3333	33.3333
G-VCL	33.3333	33.3333	33.3333	33.3333
GM-VCL	33.3333	33.3333	33.3333	33.3333
G-SFSVI	66.6667	33.3333	33.3333	33.3333
EWC	63.3333	33.3333	46.6667	33.3333
SI	33.3333	33.3333	33.3333	33.3333
AQC	66.6667	63.3333	49.6032	33.3333
NC	93.3333	63.3333	62.6984	48.2540

(b) Image task sequences

Method	CI Split MNIST	CI Split CIFAR-10	CI Split HAM-8	DI Split MNIST	DI Split CIFAR-8	DI Split HAM-6
Joint MAP training	95.1077	76.2500	43.0531	93.4338	96.6250	68.3237
Fine-tuning	19.8382	19.0400	21.9512	64.4789	89.6250	63.8068
G-VCL	25.8657	19.0100	21.6463	80.1092	92.9000	63.3071
GM-VCL	25.2141	18.9800	21.0366	77.3996	92.6000	63.6112
G-SFSVI	51.1918	32.8000	34.6563	72.5471	91.2375	63.3381
EWC	73.3744	31.9400	30.8636	82.9540	94.6625	63.8068
SI	30.2364	27.0500	21.6463	79.4063	95.0750	64.0020
AQC	92.5394	61.3100	41.6660	90.9951	96.2000	66.1442
NC	77.5334	40.2500	24.1040	89.9168	93.8000	62.2400

by the Hospital Clinic in Barcelona under CC BY-NC, and BCN20000 [21] is released by ViDIR Group, Department of Dermatology, Medical University of Vienna, also under CC BY-NC.

E. Code Availability

Documented and reproducible code is available under an MIT Licence at <https://github.com/blackblitz/bcl>.

V. CONCLUSION

We formulated continual learning based on sequential maximum a posteriori inference as a recursion of loss functions and reduced the problem to function approximation. We then proposed two coreset-free methods based on it: autodiff quadratic consolidation and neural consolidation, which use a full quadratic approximation and a neural network approximation, respectively, to approximate the previous loss function. Moreover, we showed empirically that pre-training the neural network on a similar task could significantly reduce forgetting with sequential maximum a posteriori inference methods. Neural consolidation performs the best in classical task sequences, where the input dimension is small. Autodiff quadratic consolidation consistently performs very well in image task sequences with pre-training on a similar task, achieving performance comparable to joint maximum a posteriori training in many cases. In the future, we may consider

special neural network architectures for neural consolidation as well as more applications in medical image classification, document image understanding [22] and materials science [23].

ACKNOWLEDGEMENTS

We thank Pengcheng Hao, Professor Yang Li from Tsinghua Shenzhen International Graduate School and anonymous reviewers for their feedback.

REFERENCES

- [1] M. McCloskey and N. J. Cohen, “Catastrophic interference in connectionist networks: The sequential learning problem,” *Psychology of Learning and Motivation - Advances in Research and Theory*, vol. 24, C 1989.
- [2] G. M. van de Ven, T. Tuytelaars, and A. S. Tolias, “Three types of incremental learning,” *Nature Machine Intelligence*, vol. 4, no. 12, pp. 1185–1197, 2022.
- [3] S. Farquhar and Y. Gal, *Towards robust evaluations of continual learning*, 2019. arXiv: 1805.09733.
- [4] F. Huszár, *On quadratic penalties in elastic weight consolidation*, 2017. arXiv: 1712.03847.

- [5] J. Kirkpatrick, R. Pascanu, N. Rabinowitz, J. Veness, G. Desjardins, A. A. Rusu, K. Milan, J. Quan, T. Ramalho, A. Grabska-Barwinska, D. Hassabis, C. Clopath, D. Kumaran, and R. Hadsell, "Overcoming catastrophic forgetting in neural networks," *Proceedings of the National Academy of Sciences of the United States of America*, vol. 114, no. 13, pp. 3521–3526, 2017.
- [6] F. Huszár, "Note on the quadratic penalties in elastic weight consolidation," *Proceedings of the National Academy of Sciences of the United States of America*, vol. 115, no. 11, E2496–E2497, 2018.
- [7] A. Chaudhry, P. K. Dokania, T. Ajanthan, and P. H. S. Torr, "Riemannian walk for incremental learning: Understanding forgetting and intransigence," in *Computer Vision – ECCV 2018*, V. Ferrari, M. Hebert, C. Sminchisescu, and Y. Weiss, Eds., Cham: Springer International Publishing, 2018, pp. 556–572.
- [8] F. Zenke, B. Poole, and S. Ganguli, "Continual learning through synaptic intelligence," in *Proceedings of the 34th International Conference on Machine Learning*, D. Precup and Y. W. Teh, Eds., ser. Proceedings of Machine Learning Research, vol. 70, PMLR, 2017, pp. 3987–3995.
- [9] H. Ritter, A. Botev, and D. Barber, "Online structured Laplace approximations for overcoming catastrophic forgetting," in *Advances in Neural Information Processing Systems*, S. Bengio, H. Wallach, H. Larochelle, K. Grauman, N. Cesa-Bianchi, and R. Garnett, Eds., vol. 31, Curran Associates, Inc., 2018.
- [10] C. V. Nguyen, Y. Li, T. D. Bui, and R. E. Turner, "Variational continual learning," in *International Conference on Learning Representations*, 2018.
- [11] H. Phan, A. P. Tuan, S. Nguyen, N. V. Linh, and K. Than, "Reducing catastrophic forgetting in neural networks via Gaussian mixture approximation," in *Advances in Knowledge Discovery and Data Mining*, J. Gama, T. Li, Y. Yu, E. Chen, Y. Zheng, and F. Teng, Eds., Cham: Springer International Publishing, 2022, pp. 106–117.
- [12] T. G. J. Rudner, F. B. Smith, Q. Feng, Y. W. Teh, and Y. Gal, "Continual learning via sequential function-space variational inference," in *Proceedings of the 39th International Conference on Machine Learning*, K. Chaudhuri, S. Jegelka, L. Song, C. Szepesvari, G. Niu, and S. Sabato, Eds., ser. Proceedings of Machine Learning Research, vol. 162, PMLR, 2022, pp. 18 871–18 887.
- [13] K.-Y. Lee, Y. Zhong, and Y.-X. Wang, "Do pre-trained models benefit equally in continual learning?" In *Proceedings of the IEEE/CVF Winter Conference on Applications of Computer Vision (WACV)*, 2023, pp. 6485–6493.
- [14] S. V. Mehta, D. Patil, S. Chandar, and E. Strubell, "An empirical investigation of the role of pre-training in lifelong learning," *Journal of Machine Learning Research*, vol. 24, no. 214, pp. 1–50, 2023.
- [15] W. Hu, Q. Qin, M. Wang, J. Ma, and B. Liu, "Continual learning by using information of each class holistically," vol. 35, pp. 7797–7805, 2021.
- [16] X. Li, H. Li, and L. Ma, "Continual learning of medical image classification based on feature replay," in *2022 16th IEEE International Conference on Signal Processing (ICSP)*, vol. 1, 2022, pp. 426–430.
- [17] Y. Yang, Z. Cui, J. Xu, C. Zhong, W.-S. Zheng, and R. Wang, "Continual learning with Bayesian model based on a fixed pre-trained feature extractor," *Visual Intelligence*, vol. 1, no. 1, p. 5, 2023.
- [18] F. Pedregosa, G. Varoquaux, A. Gramfort, V. Michel, B. Thirion, O. Grisel, M. Blondel, P. Prettenhofer, R. Weiss, V. Dubourg, J. Vanderplas, A. Passos, D. Cournapeau, M. Brucher, M. Perrot, and E. Duchesnay, "Scikit-learn: Machine learning in Python," *Journal of Machine Learning Research*, vol. 12, pp. 2825–2830, 2011.
- [19] J. Ansel, E. Yang, H. He, N. Gimelshein, A. Jain, M. Voznesensky, B. Bao, P. Bell, D. Berard, E. Burovski, G. Chauhan, A. Chourdia, W. Constable, A. Desmaison, Z. DeVito, E. Ellison, W. Feng, J. Gong, M. Gschwind, B. Hirsh, S. Huang, K. Kalambarkar, L. Kirsch, M. Lazos, M. Lezcano, Y. Liang, J. Liang, Y. Lu, C. Luk, B. Maher, Y. Pan, C. Puhersch, M. Reso, M. Saroufim, M. Y. Siraichi, H. Suk, M. Suo, P. Tillet, E. Wang, X. Wang, W. Wen, S. Zhang, X. Zhao, K. Zhou, R. Zou, A. Mathews, G. Chanan, P. Wu, and S. Chintala, "PyTorch 2: Faster Machine Learning Through Dynamic Python Bytecode Transformation and Graph Compilation," in *29th ACM International Conference on Architectural Support for Programming Languages and Operating Systems, Volume 2 (ASPLOS '24)*, ACM, 2024.
- [20] P. Tschandl, C. Rosendahl, and H. Kittler, "The HAM10000 dataset, a large collection of multi-source dermatoscopic images of common pigmented skin lesions," *Scientific data*, vol. 5, no. 1, pp. 1–9, 2018.
- [21] C. Hernández-Pérez, M. Combaila, S. Podlipnik, N. C. Codella, V. Rotemberg, A. C. Halpern, O. Reiter, C. Carrera, A. Barreiro, B. Helba, *et al.*, "BCN20000: Dermoscopic lesions in the wild," *Scientific Data*, vol. 11, no. 1, p. 641, 2024.
- [22] E. E. Kuruoğlu and A. S. Taylor, "Using annotations for summarizing a document image and itemizing the summary based on similar annotations," US7712028B2, 2010.
- [23] F. Saffarimiandoab, R. Mattesini, W. Fu, E. E. Kuruoğlu, and X. Zhang, "Insights on features' contribution to desalination dynamics and capacity of capacitive deionization through machine learning study," *Desalination*, vol. 515, p. 115 197, 2021.

APPENDIX A EXPERIMENT DETAILS

A. Data Preparation

For task sequences based on Iris and Wine, the dataset is split into training and testing datasets with 20% testing size, and then the training dataset into training and validation datasets with 20% validation size, so the training, validation and testing proportions are 64%, 16% and 20%, respectively. Finally, each dataset is split by class into a dataset sequence.

For EMNIST Letters, CIFAR-100 and task sequences based on MNIST and CIFAR-10, training and testing datasets are available from PyTorch, so the training dataset is split into training and validation datasets with 20% validation size. Each dataset is then split by class into a dataset sequence.

For BCN-12 and HAM-8, the 640×450 images are resized to 32×32 with Lanczos interpolation. For all image data, the pixel values are divided by 255 so that they take values between 0 and 1. Data augmentation (e.g. flipping and cropping) is not performed.

B. Neural Network Architectures

The fully connected neural network used for CI Split 2D Iris and CI Split Iris has 1 hidden layer of 4 nodes, while that used for CI Split Wine has 1 hidden layer of 16 nodes. All the hidden nodes use swish activation.

The pre-trained neural network for both CI Split MNIST and DI Split MNIST has 2 convolutional layers and 2 dense layers, totaling 4 layers. Each convolutional layer has $32 \times 3 \times 3$ filters and is followed by group normalization with 32 groups, swish activation and average pooling with a size of 2×2 . The hidden dense layer has 64 nodes with swish activation. Thus, the feature dimension is 64.

The pre-trained neural network for CI Split CIFAR-10, CI Split HAM-8 DI Split CIFAR-8 and DI Split HAM-6 has 17 convolutional layers and 1 dense layer, totaling 18 layers. Each convolutional layer is followed by group normalization with 32 groups and swish activation. The 2nd to the 17th convolutional layers are arranged into 8 residual blocks, each with 2 convolutional layers, and every 2 residual blocks are followed by average pooling with a size of 2×2 . The numbers of filters for the 17 convolutional layers are 32, 64, 64, 64, 64, 128, 128, 128, 128, 256, 256, 256, 256, 512, 512, 512 and 512, respectively, and the filter sizes are all 3×3 . Thus, the feature dimension is 512.

In all experiments, the consolidator neural network used in NC is a fully connected neural network with 2 hidden layers, each with 256 nodes. All the hidden nodes use swish activation.

C. Training

In all experiments, the prior PDF at time 1 is a standard Gaussian PDF (of an appropriate dimension), and an Adam optimizer is used with a one-cycle learning rate schedule. The neural network parameters are initialized by using the Lecun normal initializer for the weights and setting to zero for the biases. For pre-training tasks and class-incremental task

sequences, each task is of multi-class classification, so categorical cross entropy is used, while for domain-incremental task sequences, each task is of binary classification, so binary or Bernoulli cross entropy is used. BCN-12 is a task with severe class imbalance, so for pre-training on BCN-12, instead of the standard cross entropy, a weighted cross entropy $-\sum_{i=1}^k \frac{m}{n_i} p_i \ln q_i$ is used, where p_i is the true label indicator and q_i is the predicted probability, n_i is the frequency of the i -th class and $m = \min\{n_1, n_2, \dots, n_k\}$.

For CI Split 2D Iris and CI Split Iris, training for each task is performed for 100 epochs with a base learning rate of 0.1 and a batch size of 16. For CI Split Wine, training for each task is performed similarly but with a base learning rate of 0.01.

For CI Split MNIST and DI Split MNIST, pre-training is performed on EMNIST Letters for 20 epochs with a base learning rate of 0.01 and a batch size of 64, and training for each task is performed similarly. For CI Split MNIST and DI Split CIFAR-8, pre-training is performed on CIFAR-100 for 20 epochs with a base learning rate of 0.001 and a batch size of 64, and training for each task is performed similarly but with a base learning rate of 0.01. For CI Split HAM-8 and DI Split HAM-6, pre-training is performed on BCN-12 for 20 epochs with a base learning rate of 0.0001 and a batch size of 64, and training for each task is performed similarly but with a base learning rate of 0.001.

For G-SFSVI, the inducing points are randomly generated from a uniform distribution in a hyperrectangle the boundaries of which are determined by the minimum and maximum values of the training input data across all tasks in the task sequence. For image task sequences with pre-training, the boundaries for each feature component are set to -1 and 6.

D. Hyperparameter Tuning

In EWC, SI, AQC and NC, there is a hyperparameter λ that determines the regularization strength. SI has an extra damping hyperparameter ξ and NC has an extra radius hyperparameter r . Hyperparameter tuning is performed based on the validation final average accuracy via grid search among the following values:

- EWC: $\lambda \in \{1, 10, 100, 1000, 10000\}$
- SI: $\lambda \in \{1, 10, 100, 1000, 10000\}, \xi \in \{0.1, 1.0, 10\}$
- AQC: $\lambda \in \{1, 10, 100, 1000, 10000\}$
- NC: $\lambda \in \{1, 10, 100, 1000, 10000\}, r \in \{1, 10, 100\}$